Mechanism of double-base lesion bypass catalyzed by a Y-family DNA polymerase

Jessica A. Brown[1,2], Sean A. Newmister[1], Kevin A. Fiala[1,2] and Zucai Suo[1,2,3,4,5,*]

[1]Department of Biochemistry, [2]Ohio State Biochemistry Program, [3]Ohio State Biophysics Program, [4]Molecular, Cellular & Developmental Biology Program and [5]Comprehensive Cancer Center, The Ohio State University, Columbus, OH 43210, USA

ABSTRACT

As a widely used anticancer drug, *cis*-diamminedichloroplatinum(II) (cisplatin) reacts with adjacent purine bases in DNA to form predominantly *cis*-[Pt(NH$_3$)$_2${d(GpG)-N7(1),-N7(2)}] intrastrand cross-links. Drug resistance, one of the major limitations of cisplatin therapy, is partially due to the inherent ability of human Y-family DNA polymerases to perform translesion synthesis in the presence of DNA-distorting damage such as cisplatin–DNA adducts. To better understand the mechanistic basis of translesion synthesis contributing to cisplatin resistance, this study investigated the bypass of a single, site-specifically placed cisplatin-d(GpG) adduct by a model Y-family DNA polymerase, *Sulfolobus solfataricus* DNA polymerase IV (Dpo4). Dpo4 was able to bypass this double-base lesion, although, the incorporation efficiency of dCTP opposite the first and second cross-linked guanine bases was decreased by 72- and 860-fold, respectively. Moreover, the fidelity at the lesion decreased up to two orders of magnitude. The cisplatin-d(GpG) adduct affected six downstream nucleotide incorporations, but interestingly the fidelity was essentially unaltered. Biphasic kinetic analysis supported a universal kinetic mechanism for the bypass of DNA lesions catalyzed by various translesion DNA polymerases. In conclusion, if human Y-family DNA polymerases adhere to this bypass mechanism, then translesion synthesis by these error-prone enzymes is likely accountable for cisplatin resistance observed in cancer patients.

INTRODUCTION

cis-Diamminedichloroplatinum(II) (cisplatin, DDP) is a potent anticancer drug that is effective for the treatment of testicular, ovarian, head, neck, and nonsmall cell lung cancers. During the biotransformation of cisplatin *in vitro* and *in vivo*, cisplatin reacts with the N7 position of purines to generate several possible adducts: *cis*-[Pt(NH$_3$)$_2${d(GpG)-N7(1),-N7-(2)}] intrastrand cross-links (cis-platin-d(GpG)), *cis*-[Pt(NH$_3$)$_2${d(ApG)-N7(1),-N7-(2)}] intrastrand cross-links, *cis*-[Pt(NH$_3$)$_2$ {d(GpNpG)-N7(1),-N7-(3)}] intrastrand cross-links, 1,3-interstrand cross-links with guanines and monofunctional cross-links with guanine (1–4). These cisplatin–DNA adducts can severely inhibit DNA replication, thereby highlighting this cytotoxic effect as an important mode of drug action. Upon encountering a cisplatin–DNA adduct *in vitro*, replicative DNA polymerases, e.g. eukaryotic DNA polymerases α (5,6), δ (6) and ε (7), stall while most DNA repair and lesion bypass polymerases can traverse the lesion. Y-family DNA polymerases, characterized by low fidelity and processivity, are notorious for bypassing DNA lesions. Of the four Y-family members in humans, DNA polymerase η (Polη) bypasses cisplatin–DNA adducts in a relatively efficient and error-free manner *in vitro* (8–11), and cell-based assays provide additional evidence that Polη is involved in the bypass of this adduct *in vivo* (12–14). DNA polymerases ι (Polι) (15) and κ (Polκ) (16,17) are impeded by cisplatin–DNA adducts, however, it remains to be explored whether bypass is possible via the two-polymerase model of lesion bypass (18,19). Recent studies provide evidence that Rev1, both a deoxycytidyl transferase and structural factor during replication, modulates cisplatin mutagenicity (20,21), but the catalytic activity appears to be dispensable (22). Other relevant eukaryotic DNA polymerases implicated in the bypass of cisplatin–DNA adducts are DNA polymerases γ (23), ζ (23–25), β (6,10,11,26–28) and μ (29). Finally, a variety of cellular processes have been proposed to promote cancer cell survival, which contributes to clinical drug resistance associated with cisplatin. Some of these *in vivo* processes are the following: reduced drug uptake, enhanced drug inactivation, increased DNA repair, disabled apoptotic signaling machinery and translesion DNA synthesis (TLS) [see reviews in refs (30–34) for a comprehensive overview of postulated mechanisms].

Thus, to circumvent the hurdles of drug resistance and to design improved anticancer drugs, it is imperative to understand the effect of cisplatin as it pertains to lesion bypass at the molecular level.

For this study, we investigated the mechanistic basis of lesion bypass catalyzed by *Sulfolobus solfataricus* DNA polymerase IV (Dpo4) for a single, site-specifically placed cisplatin-d(GpG) adduct using pre-steady state kinetics. Utilizing this methodology, we have previously established (i) the minimal kinetic mechanism and fidelity of Dpo4 incorporating a single nucleotide into undamaged DNA (35,36) and (ii) the mechanistic basis of Dpo4 bypassing an abasic site, which is a prototype single-base lesion (37). To provide a deeper mechanistic understanding of how Y-family DNA polymerases catalyze the bypass of other DNA lesions, we used the cisplatin-d(GpG) adduct as a model double-base lesion and Dpo4 as a model Y-family DNA polymerase. Among the aforementioned cisplatin–DNA adducts, cisplatin-d(GpG) is the predominant species (∼65%) and has been correlated with clinical efficacy of the drug (2,38,39). Although Dpo4 shares more sequence similarity with Polκ as a DinB homolog, one study suggests that the lesion bypass properties of Dpo4 are more similar to Polη (40). Consequently, establishing the kinetic mechanism of Dpo4 bypassing the cisplatin-d(GpG) adduct may (i) establish the mechanistic basis of double-base lesion bypass, (ii) illuminate the molecular basis of drug resistance due to cisplatin bypass, (iii) assess the mutagenic potential of inducing secondary malignancies and (iv) enable scientists to design more effective anticancer drugs.

MATERIALS AND METHODS

Reaction buffers

Optimized reaction buffer D contains the following: 50 mM HEPES (pH 7.5 at 37°C), 5 mM MgCl$_2$, 50 mM NaCl, 5 mM DTT, 10% glycerol, 0.1 mM EDTA and 0.1 mg/ml bovine serum albumin (BSA) (36). For the gel mobility shift assay, reaction buffer E contains the following: 50 mM Tris–Cl (pH 7.5 at 23°C), 5 mM MgCl$_2$, 50 mM NaCl, 5 mM DTT, 10% glycerol and 0.1 mg/ml BSA. All reported concentrations were the final concentrations upon mixing. All reactions, unless noted, were performed at 37°C.

DNA substrates

The cisplatinated-DNA oligonucleotide (Table 1) was modified, ligated and purified previously (41). All DNA primers (Table 1) were prepared previously (41) except for the 21-mer purchased from Integrated DNA Technologies, Inc., Coralville, IA and subsequently gel purified. The DNA primers were 5′-radiolabeled with [γ-^{32}P]ATP (GE Healthcare, Picataway, NJ, USA) and Optikinase (USB) (36). To anneal, the [^{32}P]-radiolabeled DNA primer and unlabeled template were combined at a 1:1.15 molar ratio, respectively, heated to 85°C for 6 min and cooled slowly to room temperature.

Table 1. DNA sequences of primers and templates

Primers	
19-mer	5′-GTCCCTGTTCGGGCGCCAG-3′
21-mer	5′-GTCCCTGTTCGGGCGCCAGGA-3′
22-mer	5′-GTCCCTGTTCGGGCGCCAGGAG-3′
23-mer	5′-GTCCCTGTTCGGGCGCCAGGAGA-3′
24-mer	5′-GTCCCTGTTCGGGCGCCAGGAGAC-3′
25-mer	5′-GTCCCTGTTCGGGCGCCAGGAGACC-3′
26-mer	5′-GTCCCTGTTCGGGCGCCAGGAGACCA-3′
27-mer	5′-GTCCCTGTTCGGGCGCCAGGAGACCAG-3′
28-mer	5′-GTCCCTGTTCGGGCGCCAGGAGACCAGA-3′
29-mer	5′-GTCCCTGTTCGGGCGCCAGGAGACCAGAG-3′
30-mer	5′-GTCCCTGTTCGGGCGCCAGGAGACCAGAGG-3′
31-mer	5′-GTCCCTGTTCGGGCGCCAGGAGACCAGAGGC-3′
32-mer	5′-GTCCCTGTTCGGGCGCCAGGAGACCAGAGG CT-3′
Templates	
44DDP[a]	3′-CAGGGACAAGCCCGCGGTCCTCT**GG**TCTCCGAT CAGAGCACTAG-5′
44CTL	3′-CAGGGACAAGCCCGCGGTCCTCTGGTCTCCGAT CAGAGCACTAG-5′

[a]The cisplatin-modified guanines are in bold.

Running start assay

Using a rapid-chemical quench flow apparatus (KinTek), a solution of preincubated Dpo4 (100 nM) and 5′-[^{32}P] DNA (100 nM) was mixed with an equal volume (15 μl) of all four dNTPs (200 μM each) in buffer D and quenched with 0.37 M EDTA at times ranging from ms to min. The incorporation pattern was resolved via denaturing polyacrylamide gel electrophoresis (PAGE).

Electrophoretic mobility shift assay (EMSA)

To determine the K_d^{DNA} for the Dpo4•DNA binary complex, Dpo4 (15–600 nM) was added to a solution containing 5′-[^{32}P] DNA (100 nM) in buffer E and allowed to equilibrate for 15 min at 23°C. Then, the binary complex was separated from unbound DNA using a 4.5% native polyacrylamide gel with a running buffer as described previously (37) and quantitated using a PhosphorImager 445 SI (Molecular Dynamics, Sunnyvale, CA, USA). A plot of binary complex formation versus the concentration of Dpo4 was fit to Equation 1

$$[E \bullet DNA] = 0.5\big(K_d^{DNA} + E_0 + D_0\big)$$
$$- 0.5\Big[\big(K_d^{DNA} + E_0 + D_0\big)^2 - 4E_0D_0\Big]^{1/2} \quad \mathbf{1}$$

where E_0 and D_0 represent the active enzyme and DNA concentrations, respectively.

Determination of the k_p and K_d of an incoming nucleotide

A pre-equilibrated solution of Dpo4 (120 nM) and 5′-[^{32}P] DNA (30 nM) in buffer D was combined with increasing concentrations of a single dNTP (25–1600 μM) in buffer D. Aliquots of the reaction mixtures were quenched at various times using 0.37 M EDTA. For fast reaction times, a rapid-chemical quench flow apparatus was used. Reaction products were resolved using sequencing gel electrophoresis and quantitated with a PhosphorImager

445 SI. The time course of product formation at each nucleotide concentration was fit to a single-exponential equation (Equation 2) using a nonlinear regression program, KaleidaGraph (Synergy Software, Essex Junction, VT, USA).

$$[\text{Product}] = A[1 - \exp(-k_{obs}t)] \qquad \mathbf{2}$$

A represents the reaction amplitude. The extracted values for the observed rate constant (k_{obs}) of nucleotide incorporation were plotted as a function of dNTP•Mg^{2+} concentration and fit to a hyperbolic equation (Equation 3)

$$k_{obs} = k_p[\text{dNTP}]/\{[\text{dNTP}] + K_d\} \qquad \mathbf{3}$$

which resolved the k_p and K_d values for nucleotide incorporation. The substrate specificity (k_p/K_d), efficiency ratio $[(k_p/K_d)_{control}/(k_p/K_d)_{damaged}]$, and fidelity $\{(k_p/K_d)_{incorrect}/[(k_p/K_d)_{correct} + (k_p/K_d)_{incorrect}]\}$ were then calculated.

Biphasic kinetic assays

A pre-equilibrated solution of Dpo4 (120 nM) and 5'-[^{32}P] DNA (30 nM) in buffer D was mixed with a DNA trap [5 µM, 21-mer/41CTL D-1 (36)] and dNTP (1.0 mM) in buffer D supplemented with Mg^{2+}, which may be chelated by the DNA trap as previously described (37). A rapid chemical quench flow apparatus was used to quench aliquots of the reaction mixtures at various times using 0.37 M EDTA. Reaction products were resolved and quantitated as described earlier. The concentration of product formation was graphed as a function of time and fit to a double-exponential equation (Equation 4) using KaleidaGraph.

$$[\text{Product}] = E_0A_1[1 - \exp(-k_1t)] + E_0A_2[1 - \exp(-k_2t)] \qquad \mathbf{4}$$

E_0 represents the total enzyme concentration, A_1 and A_2 represent the first and second phase reaction amplitudes, respectively, and k_1 and k_2 represent the first and second phase rate constants, respectively.

RESULTS

Bypass of a cisplatin-d(GpG) adduct

We have previously constructed a 44-mer DNA template (44DDP) containing a site-specific cisplatin-d(GpG) adduct (Table 1) (41). To generate a nucleotide incorporation profile using this adduct-containing DNA substrate, we first performed a 'running start' assay (see Materials and methods section) to visualize the extension of the 5'-[^{32}P]-labeled 19-mer/44DDP (Table 1) catalyzed by Dpo4 in the presence of all four dNTPs (Figure 1B). Our results showed that Dpo4 bypassed the single cisplatin-d(GpG) adduct, as full-length product (44-mer) was detected at 60 s (Figure 1B). Although Dpo4 synthesized full-length product, the significant accumulation of intermediate products revealed two distinct pause sites (23- and 24-mers) corresponding to nucleotide incorporations opposite the cisplatin-d(GpG) adduct. In comparison, Dpo4 did not pause at these positions in the

control experiment with an undamaged DNA substrate (19-mer/44CTL, Table 1) in which full-length product was generated within 10 s (Figure 1A). The purity of 44DDP was examined to ensure that the bypass products in Figure 1B were not due to a subpopulation of unmodified or deplatinated 44-mer (Supplementary Figure 1). Also notable, the observation of 45- and 46-mer products suggested Dpo4 catalyzed template-independent nucleotide incorporations (Figure 1) (42). However, this result warrants further investigation due to the possibility of nucleotide deletions, nucleotide additions or other complex transactions occurring in the vicinity of the lesion as previously demonstrated (10,26,43–47).

Binding of Dpo4 to cisplatin-modified DNA

Various structural studies reveal a significant bend in the DNA, ∼40–80°, which may preclude binary complex formation (48–50). Since the two strong pause sites occur opposite the cisplatin-d(GpG) lesion, it is possible that a weaker binding affinity of Dpo4 to DNA may be a contributing factor. Therefore, we determined the equilibrium dissociation constant (K_d^{DNA}) of several binary complexes using the EMSA (see Materials and methods section). EMSA has been proven to be a reliable assay for estimating the K_d^{DNA} value of the Dpo4•DNA binary complex (37,42). By varying the primer length, a series of DNA substrates was designed to mimic the progression of DNA synthesis catalyzed by Dpo4 as it approached, encountered and bypassed the damaged site. For example, to measure the K_d^{DNA} value at the second pause site (Figure 1B), we titrated increasing concentrations of Dpo4 into a fixed concentration of 5'-[^{32}P]-labeled 24-mer/44DDP (Table 1). After equilibration, the binary complex Dpo4•24-mer/44DDP and free DNA were separated via native PAGE (Figure 2A). Next, the concentration of binary complex formation was plotted versus Dpo4 concentration (Figure 2B) and fit to a quadratic equation (Equation 1), which yielded a K_d^{DNA} of 26 ± 3 nM (Table 2). Similarly, the K_d^{DNA} for the Dpo4•24-mer/44CTL (Table 1) binary complex was measured to be 8 ± 1 nM, and the affinity ratio $[(K_d^{DNA})_{damaged}/(K_d^{DNA})_{control}]$ was calculated to be 3.3-fold (Table 2). Analysis of the first strong pause site (23-mer/44DDP) and the first downstream, nonpause site (25-mer/44DDP) revealed a similar effect on the K_d^{DNA} value (Table 2). Dpo4 binding upstream of the cisplatin lesion was unaffected, yet the binding affinity downstream was not restored until the second downstream site (Table 2). These modest, ∼3-fold lower affinity values indicated that the overall binding affinity of Dpo4 to a cisplatin-d(GpG) adduct was not significantly affected and was localized to the vicinity of the lesion. Furthermore, these results suggested that the association and dissociation rates of DNA from the Dpo4•DNA complex at or near the double-base lesion were not significantly altered, and the pausing of Dpo4 observed in Figure 1 was not due to the faster dissociation of the Dpo4•DNA complex. This conclusion was supported by the biphasic kinetics of nucleotide incorporations at the pause sites in the presence of a DNA trap (see Biphasic kinetics section). Thus, we
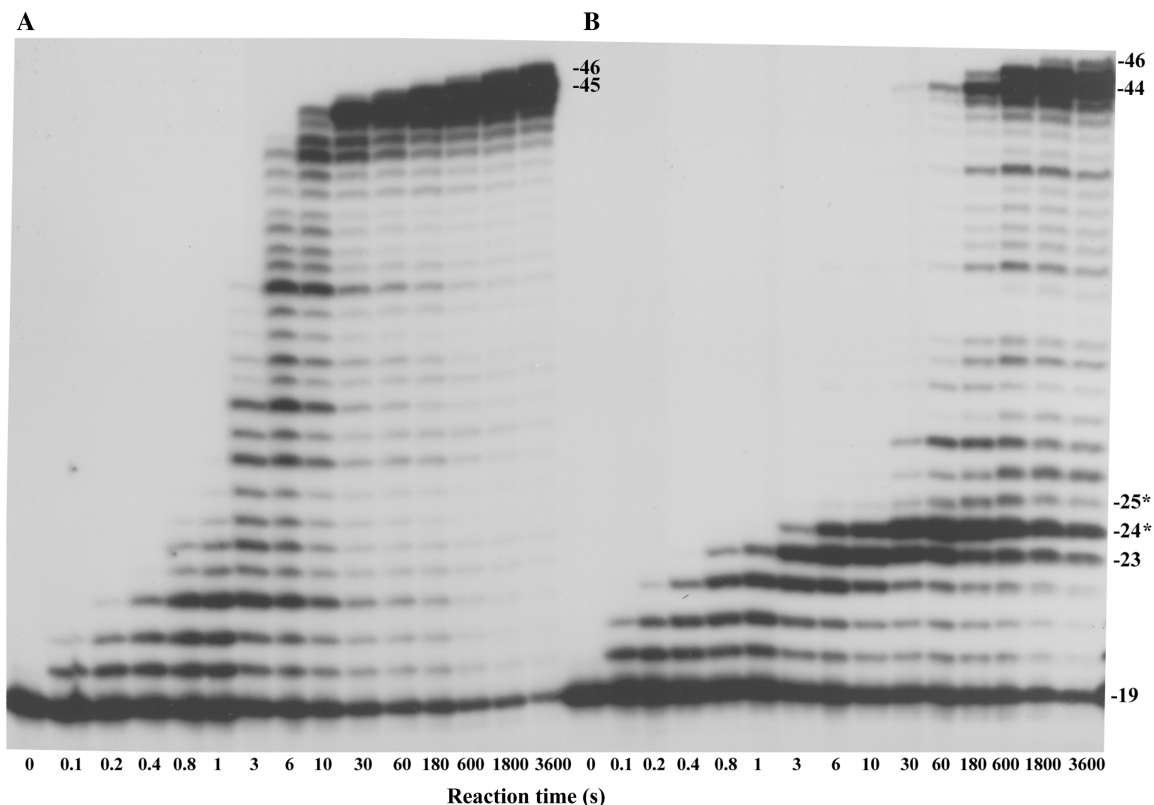
Figure 1. Running start nucleotide incorporation assay. A pre-equilibrated solution of Dpo4 (100 nM) and 5′-[^{32}P]-labeled DNA (100 nM) were mixed with all four dNTPs (200 μM each) for various reaction times before terminating with EDTA. Lengths of the resolved products and the site of the cisplatin adduct (asterisk) are designated along the right margin. (**A**) Reaction with 19-mer/44CTL substrate; (**B**) reaction with 19-mer/44DDP substrate.
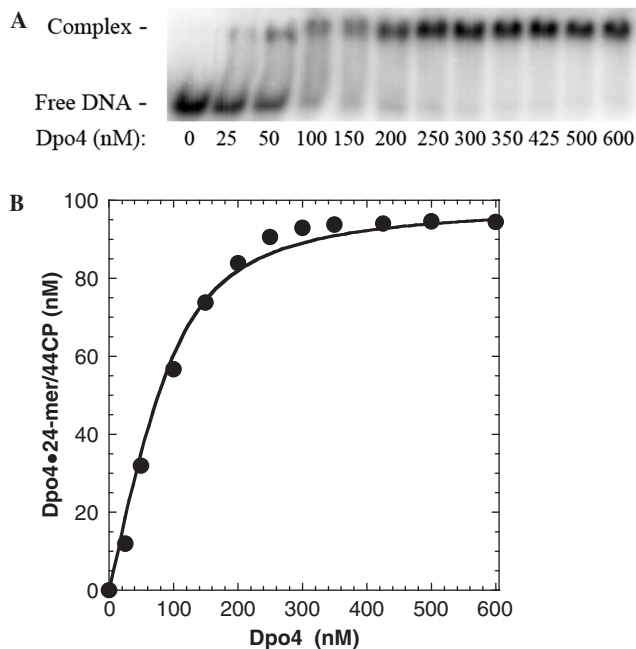

Figure 2. Measurement of Dpo4 binding to 24-mer/44DDP. (**A**) Reactions containing 5′-[^{32}P]-labeled 24-mer/44DDP (100 nM) were incubated with increasing concentrations of Dpo4 (25–600 nM). The binary complex was separated from the unbound DNA substrate via native polyacrylamide gel electrophoresis. (**B**) A plot of binary complex formation (Dpo4•24-mer/44DDP) versus Dpo4 concentration was fit to a quadratic equation (Equation 1), which yielded a K_d^{DNA} of 26 ± 3 nM.

hypothesized that the structurally distorted DNA significantly decreased the incorporation efficiency of an incoming nucleotide at the aforementioned pause sites.

Efficiency of nucleotide incorporation opposite a cisplatin-d(GpG) adduct

Transient state kinetics performed under single-turnover conditions measures the maximum incorporation rate (k_p) and the equilibrium dissociation constant (K_d) of nucleotide incorporation which are the two defining kinetic parameters of catalytic efficiency or substrate specificity (k_p/K_d). To resolve the k_p and K_d at the second pause site, a solution containing Dpo4 (120 nM) was preincubated with 5′-[^{32}P]-labeled 24-mer/44DDP (30 nM) before initiating the reaction with increasing concentrations of dCTP for various times (see Materials and methods section). A primary plot of product concentration versus time conformed to a single-exponential fit (Equation 2) so that the k_{obs} values were extracted for each dCTP concentration (Figure 3A and Supplementary Figure 2). Then, a secondary plot of the k_{obs} values versus dCTP concentration was fit to Equation 3 which yielded a k_p of 0.043 ± 0.004 s^{-1} and a K_d of 588 ± 145 μM (Figure 3B and Table 3). The calculated substrate specificity of 7.3 × 10^{-5} μM^{-1} s^{-1} was ∼860-fold lower than dCTP incorporation into undamaged 24-mer/44CTL (Tables 3 and 4). Any bias due to a DNA sequence-dependent effect was attenuated by determining the kinetic parameters for

Table 2. Binding affinity of Dpo4 to control and damaged DNA substrates at 23°C

Damaged substrate	K_d^{DNA} (nM)	Control substrate	K_d^{DNA} (nM)	Affinity ratio[a]
21-mer/44DDP	8 ± 1	21-mer/44CTL	18 ± 3	0.4-fold
22-mer/44DDP	21 ± 4	22-mer/44CTL	16 ± 3	1.3-fold
23-mer/44DDP[b]	56 ± 9	23-mer/44CTL	17 ± 2	3.3-fold
24-mer/44DDP[b]	26 ± 3	24-mer/44CTL	8 ± 1	3.3-fold
25-mer/44DDP	17 ± 4	25-mer/44CTL	5 ± 1	3.4-fold
26-mer/44DDP	12 ± 2	26-mer/44CTL	11 ± 2	1.1-fold
27-mer/44DDP	17 ± 3	27-mer/44CTL	13 ± 4	1.3-fold

[a]Calculated as $(K_d^{DNA})_{damaged}/(K_d^{DNA})_{control}$.
[b]DNA substrates at strong pause sites.

all correct incorporations into 44CTL, and these results indicated that the incorporation efficiency varied over a 30-fold range (Table 4). Furthermore, the substrate specificity for dCTP incorporation into 23-mer/44DDP was reduced by 72-fold relative to the control DNA substrate 23-mer/44CTL (Tables 3 and 4). Please note, these are apparent k_p and K_d values at the strong pause sites due to the detection of biphasic kinetics of nucleotide incorporation at these sites (see Discussion section). Misincorporation at the two strong pause sites opposite the cisplatin cross-linked guanines followed similar trends in which (i) the order of preferred dNTP incorporation was dATP > dTTP > dGTP, (ii) the k_p/K_d values were in the range of 10^{-6} to $10^{-7} \mu M^{-1} s^{-1}$ and (iii) the fidelity was in the low range of 10^{-4} to 10^{-3} at the 3′-dG site and 10^{-3} to 10^{-2} at the 5′-dG site (Table 3). Collectively, these kinetic data supported our hypothesis that a decreased nucleotide incorporation efficiency explained the significant product accumulation induced by the cisplatin–DNA adduct (Figure 1B and Table 3).

Efficiency of nucleotide incorporation proximal to the cisplatin-d(GpG) adduct

In parallel single-turnover experiments, the substrate specificity for events both upstream and downstream from the lesion was kinetically examined using a series of DNA primers with the same cisplatinated or control DNA templates (Table 1). The efficiency ratio, defined as the substrate specificity for the control DNA divided by the substrate specificity for damaged DNA, provides a foundation for our kinetic comparisons. All upstream events were essentially normal (efficiency ratios of 1.1 and 1.5), while the downstream events revealed an intriguing trend (Figure 4A). Interestingly, the incorporation efficiency did not gradually decrease as a linear function before resuming to normal. Instead, the most significant downstream perturbation occurred at the −2 and −3 positions relative to the cisplatinated 5′-dG (Table 3 and Figure 4A). At these 'weak' pause sites, the efficiency ratio for correct dNTP incorporation into 26-mer/44DDP and 27-mer/44DDP was decreased by 36- and 17-fold, respectively, but there was not a dramatic effect on fidelity (Table 3 and Figure 4B). In addition, these 'weak' pause sites were observable in the running start assay as a minor accumulation of intermediate products (26- and 27-mers) (Figure 1B). Other notable sites in which Dpo4 appeared
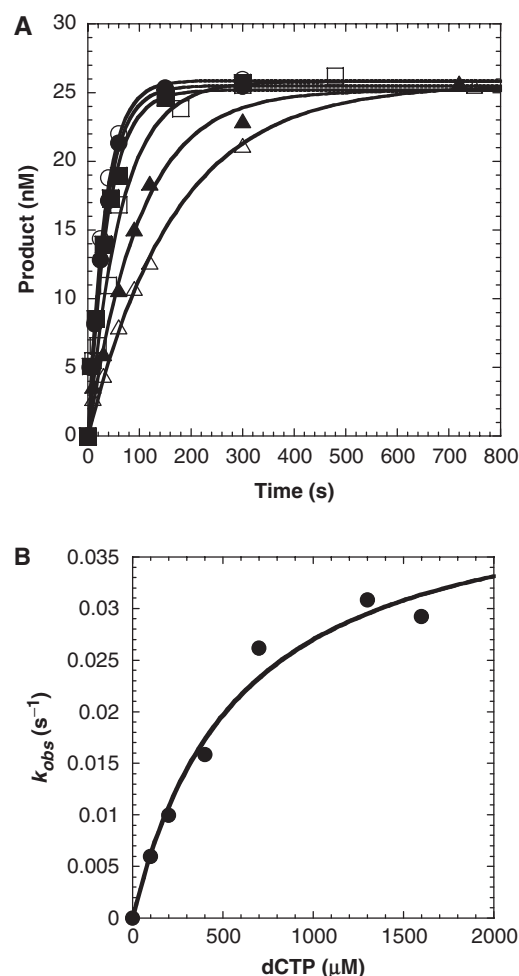

Figure 3. Concentration dependence on the pre-steady state rate constant of dCTP incorporation. A preincubated solution of Dpo4 (120 nM) and 5′-[^{32}P]-labeled 24-mer/44DDP (30 nM) was rapidly mixed with increasing concentrations of dCTP•Mg^{2+} (100 μM, open triangle; 200 μM, filled triangle; 400 μM, filled square; 700 μM, filled square; 1300 μM, open circle; 1600 μM, closed circle) for various time intervals. (**A**) The solid lines represent the best fits to a single exponential (Equation 2), which determined the observed rate constants, k_{obs}. Plots for each dCTP time course are provided in Supplementary Figure 2. (**B**) The k_{obs} values were plotted as a function of dCTP concentration and fit to a hyperbolic (Equation 3), whereby a k_p of $0.043 \pm 0.004\,s^{-1}$ and a K_d of $588 \pm 145\,\mu M$ were obtained.

to pause during dNTP incorporation include 25-mer/44DDP, 29-mer/44DDP and 30-mer/44DDP (Figure 4A). Slowing the rate of maximum nucleotide incorporation lead to a waning of the substrate specificity in an unprecedented cyclic pattern during the downstream extension steps. These observations reinforced the kinetic impact of a severely distorted DNA molecule within or near the active site of a DNA polymerase (48–50). Overall, the catalytic efficiency of Dpo4 synthesizing on a cisplatin-modified DNA substrate returned to normal after seven downstream incorporations (Table 3 and Figure 4A).

Biphasic kinetics

Biphasic kinetic analysis is useful for extracting the rate constants and amplitudes for reactions in which distinct

Table 3. Kinetic parameters of nucleotide incorporation into cisplatin-modified DNA

DNA substrate (P/T)	dNTP	$k_p{}^a$ (s^{-1})	$K_d{}^a$ (μM)	k_p/K_d (μM^{-1} s^{-1})	Efficiency ratio[b]	Fidelity[c]
21-mer/44DDP	dGTP	6.0 ± 0.2	$(2.0 \pm 0.2) \times 10^2$	3.0×10^{-2}	1.5	–
	dATP	0.026 ± 0.002	$(1.0 \pm 0.1) \times 10^3$	2.7×10^{-5}	0.97	9.1×10^{-4}
	dCTP	0.039 ± 0.007	$(6 \pm 3) \times 10^2$	6.7×10^{-5}	2.6	2.3×10^{-3}
	dTTP	0.011 ± 0.001	$(1.3 \pm 0.2) \times 10^3$	8.6×10^{-6}	1.4	2.9×10^{-4}
22-mer/44DDP	dATP	3.8 ± 0.2	$(3.9 \pm 0.7) \times 10^2$	9.8×10^{-3}	1.1	–
	dCTP	0.0041 ± 0.0004	$(1.4 \pm 0.2) \times 10^3$	2.9×10^{-6}	29	2.9×10^{-4}
	dGTP	$0.0081 \pm .0009$	$(1.1 \pm 0.2) \times 10^3$	7.1×10^{-6}	10	7.2×10^{-4}
	dTTP	0.0021 ± 0.0002	$(7 \pm 2) \times 10^2$	3.2×10^{-6}	5.5	3.3×10^{-4}
23-mer/44DDP	dCTP	1.6 ± 0.2	$(1.3 \pm 0.2) \times 10^3$	1.3×10^{-3}	72	–
	dATP	0.0056 ± 0.0005	$(7 \pm 1) \times 10^2$	8.0×10^{-6}	3.4	6.3×10^{-3}
	dGTP	0.00050 ± 0.00008	$(6 \pm 2) \times 10^2$	9.1×10^{-7}	67	7.2×10^{-4}
	dTTP	0.0017 ± 0.0003	$(6 \pm 2) \times 10^2$	2.8×10^{-6}	21	2.2×10^{-3}
24-mer/44DDP	dCTP	0.043 ± 0.004	$(6 \pm 1) \times 10^2$	7.3×10^{-5}	860	–
	dATP	0.00265 ± 0.00009	$(4.6 \pm 0.4) \times 10^2$	5.7×10^{-6}	4.7	7.3×10^{-2}
	dGTP	0.000171 ± 0.000008	$(8.0 \pm 0.8) \times 10^2$	2.1×10^{-7}	290	2.9×10^{-3}
	dTTP	0.00075 ± 0.00003	$(6.4 \pm 0.7) \times 10^2$	1.2×10^{-6}	51	1.6×10^{-2}
25-mer/44DDP	dATP	9.6 ± 0.4	$(5.8 \pm 0.6) \times 10^2$	1.6×10^{-2}	6.1	–
	dCTP	0.031 ± 0.004	$(1.6 \pm 0.3) \times 10^3$	1.9×10^{-5}	4.4	1.2×10^{-3}
	dGTP	0.0115 ± 0.0009	$(1.1 \pm 0.2) \times 10^3$	1.0×10^{-5}	6.8	6.3×10^{-4}
	dTTP	0.025 ± 0.003	$(1.3 \pm 0.2) \times 10^3$	1.9×10^{-5}	0.92	1.2×10^{-3}
26-mer/44DDP	dGTP	1.9 ± 0.1	$(4.0 \pm 0.7) \times 10^2$	4.7×10^{-3}	36	–
	dATP	0.04 ± 0.01	$(1.5 \pm 0.8) \times 10^3$	2.7×10^{-5}	0.98	5.6×10^{-3}
	dCTP	0.007 ± 0.002	$(1.4 \pm 0.5) \times 10^3$	5.0×10^{-6}	35	1.1×10^{-3}
	dTTP	0.0032 ± 0.0006	$(1.1 \pm 0.4) \times 10^3$	2.8×10^{-6}	4.3	6.0×10^{-4}
27-mer/44DDP	dATP	0.20 ± 0.02	$(2.7 \pm 0.7) \times 10^2$	7.5×10^{-4}	17	–
	dCTP	0.0016 ± 0.0003	$(8 \pm 3) \times 10^2$	2.1×10^{-6}	40	2.8×10^{-3}
28-mer/44DDP	dGTP	4.4 ± 0.3	$(5.0 \pm 0.9) \times 10^2$	8.9×10^{-3}	2.8	–
	dATP	0.0057 ± 0.0006	$(1.5 \pm 0.3) \times 10^3$	3.9×10^{-6}	6.7	4.3×10^{-4}
29-mer/44DDP	dGTP	0.72 ± 0.05	$(5.0 \pm 0.9) \times 10^2$	1.4×10^{-3}	4.0	–
	dATP	0.0016 ± 0.0001	$(6 \pm 1) \times 10^2$	2.8×10^{-6}	9.4	1.9×10^{-3}
30-mer/44DDP	dCTP	3.3 ± 0.2	$(2.7 \pm 0.4) \times 10^2$	1.2×10^{-2}	7.1	–
	dGTP	$0.0022 \pm .0002$	$(9 \pm 2) \times 10^2$	2.5×10^{-6}	25	2.0×10^{-4}
31-mer/44DDP	dTTP	5.5 ± 0.3	$(1.5 \pm 0.3) \times 10^2$	3.7×10^{-2}	2.1	–
	dCTP	0.019 ± 0.003	$(1.0 \pm 0.3) \times 10^3$	1.8×10^{-5}	0.69	4.9×10^{-4}
32-mer/44DDP	dATP	18.9 ± 0.8	$(1.3 \pm 0.2) \times 10^2$	1.5×10^{-1}	0.53	–
	dCTP	0.032 ± 0.002	$(8 \pm 1) \times 10^2$	3.9×10^{-5}	2.2	2.6×10^{-4}

[a]The k_p and K_d obtained with 23-mer/44DDP and 24-mer/44DDP are apparent kinetic parameters due to biphasic kinetics of nucleotide incorporations at these pause sites.
[b]Calculated as $(k_p/K_d)_{control}/(k_p/K_d)_{damaged}$ in which the $(k_p/K_d)_{control}$ is derived from Table 4 or ref. (36) for correct and incorrect incorporations, respectively.
[c]Calculated as $(k_p/K_d)_{incorrect}/[(k_p/K_d)_{correct} + (k_p/K_d)_{incorrect}]$.

Table 4. Kinetic parameters of correct nucleotide incorporation into the 44CTL DNA template

DNA substrate (P/T)	dNTP	k_p (s^{-1})	K_d (μM)	k_p/K_d (μM^{-1} s^{-1})
21-mer/44CTL	dGTP	9.3 ± 0.2	$(2.1 \pm 0.2) \times 10^2$	4.5×10^{-2}
22-mer/44CTL	dATP	4.1 ± 0.1	$(3.8 \pm 0.4) \times 10^2$	1.1×10^{-2}
23-mer/44CTL	dCTP	10.8 ± 0.4	$(1.2 \pm 0.1) \times 10^2$	9.3×10^{-2}
24-mer/44CTL	dCTP	4.5 ± 0.2	$(7 \pm 2) \times 10^1$	6.3×10^{-2}
25-mer/44CTL	dATP	15.4 ± 0.8	$(1.6 \pm 0.3) \times 10^2$	9.7×10^{-2}
26-mer/44CTL	dGTP	9.3 ± 0.2	$(5.5 \pm 0.4) \times 10^1$	1.7×10^{-1}
27-mer/44CTL	dATP	5.8 ± 0.2	$(4.0 \pm 0.5) \times 10^2$	1.3×10^{-2}
28-mer/44CTL	dGTP	15.0 ± 0.8	$(6.1 \pm 0.8) \times 10^2$	2.5×10^{-2}
29-mer/44CTL	dGTP	5.2 ± 0.5	$(9 \pm 2) \times 10^2$	5.6×10^{-3}
30-mer/44CTL	dCTP	14.5 ± 0.9	$(1.7 \pm 0.3) \times 10^2$	8.5×10^{-2}
31-mer/44CTL	dTTP	15.7 ± 0.9	$(2.0 \pm 0.4) \times 10^2$	7.7×10^{-2}
32-mer/44CTL	dATP	21 ± 1	$(2.6 \pm 0.4) \times 10^2$	8.0×10^{-2}

phases may be hidden during dNTP incorporation due to the inability to isolate different DNA polymerase binding modes (37,41). The amplitude of the first phase represents the fraction of E•DNA bound in a productive mode, whereas the amplitude of the second phase represents the nonproductively bound fraction that is slowly converted into a productive mode (Scheme 1) (37,41). Thus, examining biphasic kinetics advances our mechanistic understanding of the events occurring at the active site of a Y-family DNA polymerase upon encountering a cisplatin–DNA adduct. To perform this assay, a preincubated solution of Dpo4 (120 nM) and 5′-[^{32}P]-labeled 23-mer/44DDP (30 nM) was mixed with a solution of 21-mer/41CTL D-1 DNA trap (5 μM) and dCTP•Mg^{2+} (1.0 mM) for various times before being quenched with 0.37 M EDTA (see Materials and methods section). The purpose of the unlabeled D-1 trap is to sequester any Dpo4 molecules that dissociate from the damaged DNA substrate so that product formation is solely due to a single-binding event. The effectiveness of the D-1 DNA trap was tested and confirmed to be sufficient (see Supplementary Figure 3). A plot of product concentration as a function of time (Figure 5) was fit to Equation 4, which yielded the following kinetic parameters: $A_1 = 2.1 \pm 0.1$ nM (7%), $k_1 = 10 \pm 2$ s^{-1}, $A_2 = 19 \pm 1$ nM (63%), $k_2 = 0.0009 \pm 0.0001$ s^{-1} (Table 5). Indeed,
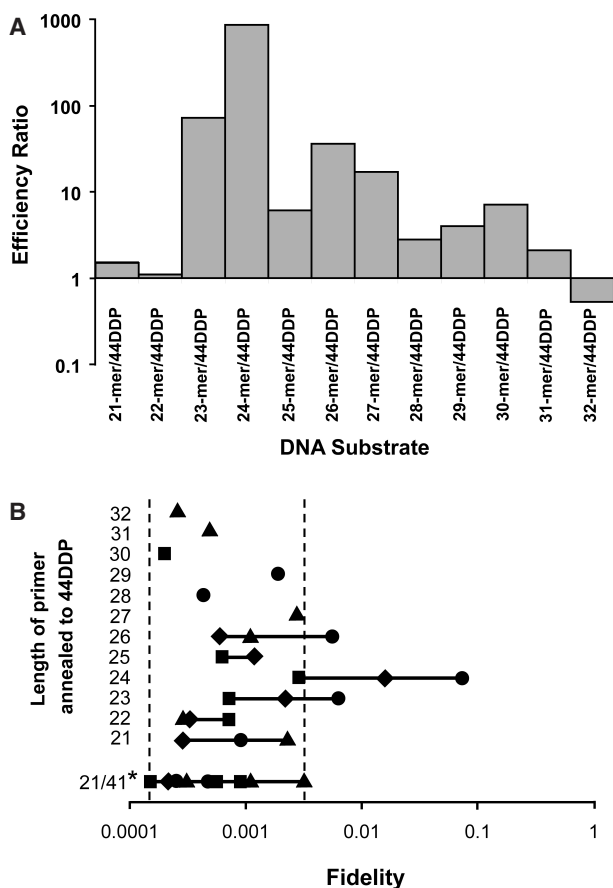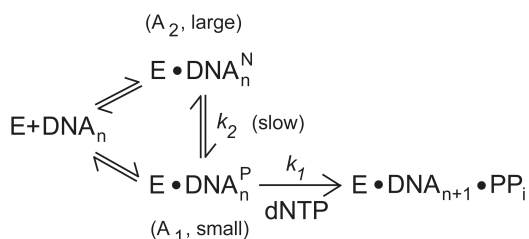
Figure 4. Quantitative effect of the cisplatin–DNA adduct on nucleotide incorporation and fidelity. (**A**) A plot of the efficiency ratio (extracted from Table 3) for each correct incorporation into DNA substrates with varying primer lengths is shown. (**B**) The fidelity of all misincorporations into undamaged [bottom most row, from ref. (36)] and damaged (upper rows) DNA by Dpo4 are shown. The two dashed vertical lines represent the outermost limits of 'normal' misincorporations by Dpo4. Each shape designates a specific dNTP: dATP, filled circle; dCTP, filled triangle; dGTP, filled square; dTTP, filled diamond. Asterisks indicate values from ref. (36).

Scheme 1.

Figure 5. Biphasic kinetics observed in the presence of a DNA trap when Dpo4 incorporated dCTP opposite the cisplatin lesion. A preincubated solution of Dpo4 (120 nM) and 5′-[^{32}P]-labeled DNA (30 nM) was rapidly mixed with 1.0 mM dCTP•Mg^{2+} in the presence of a DNA trap (5 μM) for various time intervals. Applying a double exponential (Equation 4) to a plot of product concentration versus time resolved the fast and slow phase amplitudes and rate constants for 23-mer/44DDP (filled square) and 24-mer/44DDP (filled circle). For 23-mer/44DDP, the following kinetic parameters were extracted: $A_1 = 2.1 \pm 0.1$ nM (7%), $k_1 = 10 \pm 2$ s^{-1}, $A_2 = 19 \pm 1$ nM (63%), $k_2 = 0.0009 \pm 0.0001$ s^{-1}. For 24-mer/44DDP, the following kinetic parameters were resolved: $A_1 = 1.11 \pm 0.01$ nM (3.7%), $k_1 = 4.0 \pm 0.7$ s^{-1}, $A_2 = 3.2 \pm 0.4$ nM (11%), $k_2 = 0.00016 \pm 0.00003$ s^{-1}. The inset shows product formation within 15 s, which corresponds to the fast phase.

biphasic kinetics was observed at the cisplatin cross-linked 3′-dG, whereby nucleotide incorporation initially proceeded with a fast phase of low amplitude followed by a slow phase of large amplitude. It is conceivable that the fast phase was due to unmodified or deplatinated 44-mer; however, this is unlikely because (i) 44DDP has been purified to apparent homogeneity (Supplementary Figure 1) and (ii) platinum adducts are stable under harsh temperature and pH conditions (51). Interestingly, a
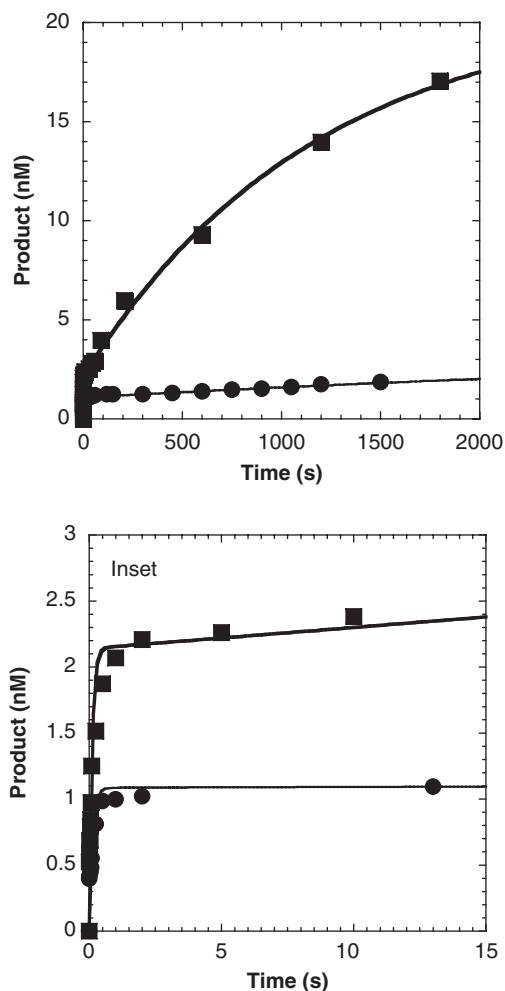
different biphasic trend emerged at the second strong pause site as evident by these kinetic values: $A_1 = 1.11 \pm 0.01$ nM (3.7%), $k_1 = 4.0 \pm 0.7$ s^{-1}, $A_2 = 3.2 \pm 0.4$ nM (11%), $k_2 = 0.00016 \pm 0.00003$ s^{-1} (Table 5 and Figure 5). These results indicated that a minute portion of Dpo4 rapidly incorporated dCTP into the Dpo4•24-mer/44DDP complex, while most of Dpo4 either dissociated or failed to achieve a catalytically competent complex. Thus, these biphasic kinetic assays provided a basis for explaining the more significant reduction in catalytic efficiency (72- versus 860-fold) for the two strong pause sites. As proof of principle, nucleotide incorporation into a nonpause site, 21-mer/44DDP, exhibited a single fast

Table 5. Biphasic kinetic parameters of dCTP incorporation into cisplatin-modified DNA

DNA substrate (P/T)	k_1 (s^{-1})	A$_1$ (nM)	k_2 (s^{-1})	A$_2$ (nM)
23-mer/44DDP	10 ± 2	2.1 ± 0.1 (7%)	0.0009 ± 0.0001	19 ± 1 (63%)
24-mer/44DDP	4.0 ± 0.7	1.11 ± 0.01 (3.7%)	0.00016 ± 0.00003	3.2 ± 0.4 (11%)

phase with a rate constant of $5.7 \pm 0.6\,\text{s}^{-1}$ in the presence of an unlabeled DNA trap (data not shown).

DISCUSSION

Kinetic basis of cisplatin resistance mediated by a Y-family DNA polymerase

The clinical effectiveness of cisplatin chemotherapy is limited by drug resistance in which the process of TLS is a likely factor (21,24,25,52,53). The newly discovered Y-family DNA polymerases are suspected to participate in the bypass of platinated-DNA adducts (5–7). Of the four human Y-family polymerases, Polη is the likely candidate responsible for bypassing platinated-DNA adducts *in vivo* (13,14). Interestingly, results from P. Blum's laboratory showed that a Dpo4-knockout cell line of *S. solfataricus* is more sensitive to cisplatin treatment than the wild-type strain (personal communication). This suggested that Dpo4, the lone Y-family DNA polymerase in *S. solfataricus*, participates in the resistance of cisplatin *in vivo*. To explore the kinetic basis of cisplatin resistance caused by the Y-family enzyme and to better understand double-base lesion bypass, we investigated the bypass of a site-specifically placed cisplatin-d(GpG) adduct catalyzed by Dpo4. Consistent with the *in vivo* observation, Figure 1B showed that Dpo4 was able to incorporate nucleotides opposite and extend from the cisplatin-d(GpG) adduct. However, the observation of intermediate product accumulation ignited further interest into elucidating the mechanistic basis of Dpo4 pausing during the insertion step as well as the lack of significant pausing during the downstream extension steps.

X-ray and NMR structural studies reveal numerous distortions when cisplatin forms a covalent linkage with two neighboring guanines in duplex DNA (48–50). Notable structural consequences in accommodating an intrastrand cross-link include the following: (i) DNA is significantly bent (~40–80°) over several base pairs, (ii) the minor groove is widened and flattened, (iii) there is a 26–49° dihedral angle between coordinated d(GpG) bases, (iv) the platinum atom is displaced from the guanine plane by ~1 Å, (v) A- and B-forms of DNA are observed, (vi) the d(GpG) bases are propeller twisted yet maintain Watson–Crick hydrogen bonding with the complementary strand and (vii) the amine group of cisplatin is hydrogen bonded to the phosphate oxygen of the DNA backbone (49,50). Despite the distorted DNA structure, the binding affinity of the binary complex was only modestly weakened (~3-fold) at the lesion site and one base downstream of the lesion (Table 2). Instead, DNA structural perturbations had a more profound effect on nucleotide incorporation efficiency and fidelity.

All incorporation events upstream of the lesion were catalyzed by Dpo4 with an efficiency comparable to undamaged DNA (Table 3). Upon encountering the cisplatin-coordinated 3′-dG, Dpo4 correctly inserted dCTP with a 72-fold decrease in efficiency relative to an undamaged dG base (Tables 3 and 4). The kinetic parameters suggested that weak dCTP binding (11-fold) accounted more for the reduction of catalytic efficiency than did the rate of dCTP incorporation (7-fold). However, the substrate specificity of dCTP incorporation at the cisplatin-coordinated 5′-dG was decreased by 860-fold due to a decrease in the rate of incorporation by 105-fold ($4.5\,\text{s}^{-1} \rightarrow 0.043\,\text{s}^{-1}$) (Tables 3 and 4). The weak apparent ground-state binding affinity ($1/K_d$) of dCTP at both strong pause sites may indicate poor base stacking. Using pyrene nucleoside 5′-triphosphate, we have shown previously that base stacking governs the binding affinity of a nucleotide opposite an abasic site (37), undamaged DNA of a recessed primer/template substrate (42) and undamaged DNA of a blunt-end substrate (42). Due to the covalent linkage of *cis*-diammineplatinum(II) with the adjacent guanine residues, the orientation of dCTP, the templating base and the 3′-OH may preclude normal base stacking interactions, thereby weakening the binding affinity of an incoming nucleotide.

Interestingly, as we completed our kinetic studies reported here, an X-ray crystallographic study of yeast Polη (yPolη) in the presence of a cisplatin-d(GpG) intrastrand cross-link and dCTP or dATP was published (54). This study provided a structural basis for the two aforementioned slow translesion steps: the incoming nucleotide's distance from the 3′-OH of the modeled primer terminus is unfavorably long (5 Å and 7.5 Å for the first and second elongation steps, respectively) (54). However, the inefficient bypass catalyzed by Dpo4 may originate from a different combination of subtle structural factors. Further kinetic analysis uncovered two distinct kinetic phases occurring at the active site of Dpo4 in the presence of a DNA trap. Bypassing the cisplatin cross-linked 3′-dG showed the rapid incorporation ($10\,\text{s}^{-1}$) of dCTP for a small percentage (7%) of the Dpo4•23-mer/44DDP complexes and then a larger percentage (63%) gradually turned over ($0.0009\,\text{s}^{-1}$) to product (Table 5 and Figure 5). These results suggested the existence of two distinct binary complexes: $E•D_n^P$ (productive) and $E•D_n^N$ (nonproductive) (Scheme 1). Initially, 7% of the Dpo4-bound species achieved a productive binary complex that was competent for catalysis, while 63% existed as a nonproductive binary complex that slowly converted into a productive state without dissociating (Table 5 and Figure 5). For the remaining 30%, which did not generate product, these Dpo4-bound species were either arrested in a 'dead-end' state or simply dissociated and diluted by the nonradiolabeled DNA trap. Structural evidence of yPolη in a pre-elongation and elongation ternary complex at the cisplatin-coordinated 3′-dG position supports the existence of the nonproductive and productive modes,

respectively, described by the kinetic data herein (54). Unfortunately, the biphasic kinetic assay cannot distinguish between the presence of binary and ternary complexes in a productive or nonproductive state due to the rapid binding of an incoming nucleotide. Thus, in light of the ternary species observed in the X-ray crystal structures of yPolη, the kinetic scheme derived from biphasic kinetic analysis (Scheme 1) has been expanded to include the possible existence of productive and nonproductive ternary complexes as shown in Supplementary Scheme 1 (54). Lastly, it is possible that there is a heterogeneous mixture of various nonproductive binding modes as binary and/or ternary complexes.

The biphasic kinetic trace during the bypass of the cisplatin-coordinated 5′-dG revealed a different trend than the cisplatin-coordinated 3′-dG as catalyzed by Dpo4 (Table 5 and Figure 5). Although dCTP was still rapidly incorporated $(4\,s^{-1})$ by a small percentage (3.7%) of productively bound Dpo4 species, a greater percentage (∼96%) was either present as a nonproductive binary complex (11%) or dissociated in favor of binding to the nonradiolabeled DNA trap (85%) (Table 5 and Figure 5). HIV type 1 reverse transcriptase (HIV-1 RT), an enzyme with low fidelity and processivity, exhibits a similar biphasic kinetic trend as Dpo4 in which the total amplitude for the first (∼25%) cross-linked guanine is greater than the second (∼2%) (41). In contrast, the total amplitudes for an exonuclease-deficient mutant of T7 DNA polymerase (T7 exo⁻) were 2.6%, 3.0% and 4.6% for correct nucleotide incorporation into 23-mer/44DDP, 24-mer/44DDP, and 25-mer/44DDP, respectively (41). Together, these biphasic kinetic data illustrate the spectrum of cisplatin-d(GpG) bypass in which the rigid active site of a replicative polymerase (e.g. T7 exo⁻) is blocked, while flexible active sites are more suitable for TLS (e.g. Dpo4 and HIV-1 RT). Despite possessing flexible active sites, not all human Y-family polymerases can independently bypass a cisplatin–DNA adduct *in vitro* (8–11,15–17). Thus, active site flexibility does not insure lesion bypass. Presumably, the flexible active site of Polη can readily accommodate productive binary and/or ternary complex formation, while the active sites of Polι and Polκ fail to achieve proper alignment for nucleotidyl transfer. Interestingly, the same mechanism shown in Scheme 1 occurs during the bypass of an abasic site, a model single-base lesion, catalyzed by Dpo4 (37). Thus, Scheme 1 or Supplementary Scheme 1 represents a universal kinetic mechanism for the bypass of single-base and double-base DNA lesions catalyzed by a variety of translesion DNA polymerases including the Y-family enzymes and HIV-1 RT.

From the overall reaction rate measured under single-turnover conditions, the individual contribution of the productive and nonproductive binary complexes can be extracted, since product formation under single-turnover conditions is comprised of all productive and nonproductive binding states. For example, opposite the cisplatin cross-linked 3′-dG, contributions from the fast phase of nucleotide incorporation $[(10\,s^{-1}) \times (7\%$ reaction amplitude)] and the slow phase $[(0.0009\,s^{-1}) \times (63\%$ reaction amplitude)] are predicted to yield an overall product

formation rate of $0.70\,s^{-1}$. Since the biphasic kinetic assays in Figure 5 were performed at sub-saturating concentrations of dCTP (1.0 mM), the observed rate at the first strong pause site was calculated to be $0.70\,s^{-1}$ based on the apparent k_p and K_d values for dCTP (Table 3) substituted into Equation 3. This value of $0.70\,s^{-1}$ matched $0.70\,s^{-1}$ estimated from the biphasic kinetic parameters. Thus, the observed rate constant extracted from single-turnover kinetic analyses was dominated by the rate constant of the fast phase, k_1. A similar connection between single-turnover and biphasic kinetic assays was obtained for abasic lesion bypass (37). Due to the complication of at least two phases occurring within a single turnover, an apparent rate of nucleotide incorporation and an apparent equilibrium dissociation constant of an incoming nucleotide was obtained at the strong pause sites (Table 3). An advantage of the biphasic kinetic assay is that the fast and slow phases can be discerned in the presence of a DNA trap. Thus, the combination of single-turnover experiments and the DNA trap assay is a powerful approach to elucidate the detailed kinetic mechanisms of lesion bypass.

To complete the TLS process, Dpo4 was able to extend the primer beyond the lesion, although there were downstream events in which Dpo4 appeared to pause slightly. These 'weak' pause sites appeared when incorporating dNTPs 1, 2, 3, 5 and 6 positions downstream from the cisplatin-coordinated 5′-dG (Figures 1B and 4A). Differential domain interactions of Dpo4 with the damaged DNA substrate may account for this unusual cyclic pattern. For instance, the little finger, thumb and/or linker region may be orienting the cisplatinated DNA into the most stable conformation, but the templating base within the active site interior may not be properly aligned for nucleotidyl transfer. As the DNA helix turns and the distance between the lesion and the Dpo4 active site increases, this downstream effect eventually dissipated after seven nucleotide incorporations (Table 3 and Figure 4A).

Steady-state kinetic data show that human Polη efficiently inserts dCTP opposite cisplatin-d(GpG) adducts, but the extension step is impaired (8,11). In contrast, human Polι and Polκ are inhibited by a cisplatin-d(GpG) adduct (15–17). Dpo4 exhibited a different pattern during TLS in which the efficiency of dCTP insertion was decreased, particularly at the cisplatin-coordinated 5′-dG lesion and the subsequent extension step was only modestly reduced (Table 3). Notably, Dpo4 seemingly behaved as a hybrid of human Polι, Polκ and Polη: Dpo4 catalyzed synthesis was problematic at the lesion similar to Polι and Polκ yet paused during the extension period like Polη (8,11,15–17).

Mutagenic potential of a cisplatin-d(GpG) adduct

Several groups have investigated the mutational spectra of cisplatin in eukaryotic cell-based assays as well as *in vivo* (43–47). At cisplatin-d(GpG) cross-links, some highlights of the reported mutation spectra include: (i) single-base substitutions, insertions and deletions, (ii) G:C → A:T transitions and G:C → T:C transversions and (iii) most of the mutagenic events were located opposite the lesion

(45–47). These results suggest that the overall TLS process by human DNA polymerases is error-prone in the presence of cisplatin-damaged DNA, although, individual DNA polymerases (e.g. Polη) may replicate in an error-free manner. For the model Y-family polymerase, the likelihood of misincorporation increased, as the fidelity of Dpo4 decreased up to two orders of magnitude when compared to the fidelity studies of normal DNA (Figure 4B) (36). For both cisplatin cross-linked guanines, dATP was promiscuously inserted (Table 3). This preferential misinsertion of dATP over dTTP and dGTP may be due to a hydrogen bond between the C6 amino group of dATP and the C6 carbonyl oxygen of cisplatin-dG. This observation is depicted in the cisplatin-coordinated 5′-dG elongation structure of yPolη with dATP (54). In regards to substrate specificity, Dpo4 selectively incorporated dCTP over dATP by 163- and 13-fold against the cisplatin-coordinated 3′-dG and 5′-dG, respectively (Table 3). Fidelity during the extension steps was relatively normal except for the 'weak' pause site at 26-mer/44DDP, whereby dATP was preferentially incorporated over the other incorrect dNTPs opposite template dC (Table 3 and Figure 4). Typically with an undamaged DNA substrate, Dpo4 discriminates between dGTP and dATP opposite template dC by 2100-fold (36); however, a discrimination factor of only 170-fold was achieved with 26-mer/44DDP (Table 3). Interestingly, the 5′ template base is dT which may explain the preferential selection of dATP. In general, the promiscuity of Dpo4 appeared to be confined to the site of the lesion, as downstream events were essentially error-free (Table 3 and Figure 4B). More importantly, this result suggested that human Y-family DNA polymerases may generate mutations during cisplatin bypass, thereby promoting the risk of secondary malignancies observed in cisplatin-treated cancer patients.

The misinsertion frequency of Dpo4 on a cisplatin-d(GpG) substrate quantitatively suggested that the overall bypass process was potentially error-prone. Although the fidelity of a DNA polymerase may be less stringent at the cisplatin-d(GpG) lesion, such as what we have observed with Dpo4, other repair pathways may compensate by preferentially recognizing misincorporations opposite the cisplatin-d(GpG) cross-link. For example, the mismatch repair complex preferentially distinguishes a mismatch depending on the base pair opposite the lesion (dT > dG > dA) as well as the type of cisplatin–DNA adduct [cisplatin-d(GpG) > cisplatin-d(ApG) > cisplatin-d(GpNpG) (55,56)]. Thus, in the presence of ciplatin, the overall integrity of genomic DNA is a complex function of several different cellular pathways.

Kinetic comparison of double-base lesion bypass

Using pre-steady state kinetics, the mechanism of correct nucleotide incorporation opposite a *cis-syn* thymine–thymine (TT) dimer catalyzed by yPolη is kinetically efficient, which is in contrast to the bypass mechanism of cisplatin-d(GpG) catalyzed by Dpo4 presented here (57). Relative to undamaged DNA, the substrate specificity for correct dNTP insertion opposite cisplatin-d(GpG) is decreased 72- to 860-fold (i.e. inefficient) for Dpo4

versus 1.2- to 6-fold (i.e. efficient) for the TT lesion and yPolη (Table 3) (57). However, binary complex formation was not significantly weakened for either enzyme despite the lesion-induced structural perturbations of the DNA helix (Table 2) (48–50,57,58). Examination of the crystal structures containing the DNA lesion in complex with a polymerase and dNTP suggest hydrogen bonding is a critical factor during TLS (54,59). Further kinetic and structural evidence is a requisite in order to fully understand the differences in the bypass efficiency and accuracy of a TT dimer and a cisplatin-d(GpG) adduct. Since yPolη is dramatically more efficient at bypassing a TT lesion, the productively bound ternary complex in Scheme 1 is likely dominant over the nonproductively bound ternary complex during TLS.

In summary, this study elucidated the kinetic mechanism of Dpo4 bypassing an important double-base lesion: a cisplatin-d(GpG) intrastrand cross-link. Although Dpo4 was capable of bypassing this double-base lesion at 37°C, the TLS process was kinetically characterized as relatively inefficient and error-prone, especially opposite the cisplatin-coordinated 5′-dG. Using the knowledge gleaned from this study, improved platinum-based anticancer drugs may be rationally designed.

SUPPLEMENTARY DATA

Supplementary Data are available at NAR Online.

REFERENCES

1. Eastman,A. (1983) Characterization of the adducts produced in DNA by cis-diamminedichloroplatinum(II) and cis-dichloro(ethylenediamine)platinum(II). *Biochemistry*, **22**, 3927–3933.
2. Fichtinger-Schepman,A. M., van der Veer,J.L., den Hartog,J.H., Lohman,P.H. and Reedijk,J. (1985) Adducts of the antitumor drug cis-diamminedichloroplatinum(II) with DNA: formation, identification, and quantitation. *Biochemistry*, **24**, 707–713.
3. Fichtinger-Schepman,A.M., van Oosterom,A.T., Lohman,P.H. and Berends,F. (1987) cis-Diamminedichloroplatinum(II)-induced DNA adducts in peripheral leukocytes from seven cancer patients: quantitative immunochemical detection of the adduct induction and removal after a single dose of cis-diamminedichloroplatinum(II). *Cancer Res.*, **47**, 3000–3004.
4. Dijt,F.J., Fichtinger-Schepman,A.M., Berends,F. and Reedijk,J. (1988) Formation and repair of cisplatin-induced adducts to DNA in cultured normal and repair-deficient human fibroblasts. *Cancer Res.*, **48**, 6058–6062.

5. Villani,G., Hubscher,U. and Butour,J.L. (1988) Sites of termination of in vitro DNA synthesis on cis-diamminedichloroplatinum(II) treated single-stranded DNA: a comparison between E. coli DNA polymerase I and eucaryotic DNA polymerases alpha. *Nucleic Acids Res.*, **16**, 4407–4418.

6. Hoffmann,J.S., Pillaire,M.J., Maga,G., Podust,V., Hubscher,U. and Villani,G. (1995) DNA polymerase beta bypasses in vitro a single d(GpG)-cisplatin adduct placed on codon 13 of the HRAS gene. *Proc. Natl Acad. Sci. USA*, **92**, 5356–5360.

7. Huang,L., Turchi,J.J., Wahl,A.F. and Bambara,R.A. (1993) Effects of the anticancer drug cis-diamminedichloroplatinum(II) on the activities of calf thymus DNA polymerase epsilon. *Biochemistry*, **32**, 841–848.

8. Vaisman,A., Masutani,C., Hanaoka,F. and Chaney,S.G. (2000) Efficient translesion replication past oxaliplatin and cisplatin GpG adducts by human DNA polymerase eta. *Biochemistry*, **39**, 4575–4580.

9. Masutani,C., Kusumoto,R., Iwai,S. and Hanaoka,F. (2000) Mechanisms of accurate translesion synthesis by human polymerase eta. *EMBO J.*, **19**, 3100–3109.

10. Bassett,E., Vaisman,A., Tropea,K.A., McCall,C.M., Masutani,C., Hanaoka,F. and Chaney,S.G. (2002) Frameshifts and deletions during in vitro translesion synthesis past Pt-DNA adducts by DNA polymerases beta and eta. *DNA Repair*, **1**, 1003–1116.

11. Bassett,E., Vaisman,A., Havener,J.M., Masutani,C., Hanaoka,F. and Chaney,S.G. (2003) Efficiency of extension of mismatched primer termini across from cisplatin and oxaliplatin adducts by human DNA polymerases beta and eta in vitro. *Biochemistry*, **42**, 14197–14206.

12. Yamada,K., Takezawa,J. and Ezaki,O. (2003) Translesion replication in cisplatin-treated xeroderma pigmentosum variant cells is also caffeine-sensitive: features of the error-prone DNA polymerase(s) involved in UV-mutagenesis. *DNA Repair*, **2**, 909–924.

13. Bassett,E., King,N.M., Bryant,M.F., Hector,S., Pendyala,L., Chaney,S.G. and Cordeiro-Stone,M. (2004) The role of DNA polymerase eta in translesion synthesis past platinum-DNA adducts in human fibroblasts. *Cancer Res.*, **64**, 6469–6475.

14. Albertella,M.R., Green,C.M., Lehmann,A.R. and O'Connor,M.J. (2005) A role for polymerase eta in the cellular tolerance to cisplatin-induced damage. *Cancer Res.*, **65**, 9799–9806.

15. McDonald,J.P., Tissier,A., Frank,E.G., Iwai,S., Hanaoka,F. and Woodgate,R. (2001) DNA polymerase iota and related rad30-like enzymes. *Philos. Trans. R. Soc. Lond. B Biol. Sci.*, **356**, 53–60.

16. Ohashi,E., Ogi,T., Kusumoto,R., Iwai,S., Masutani,C., Hanaoka,F. and Ohmori,H. (2000) Error-prone bypass of certain DNA lesions by the human DNA polymerase kappa. *Genes Dev.*, **14**, 1589–1594.

17. Gerlach,V.L., Feaver,W.J., Fischhaber,P.L. and Friedberg,E.C. (2001) Purification and characterization of pol kappa, a DNA polymerase encoded by the human DINB1 gene. *J. Biol. Chem.*, **276**, 92–98.

18. Guo,D., Wu,X., Rajpal,D. K., Taylor,J.S. and Wang,Z. (2001) Translesion synthesis by yeast DNA polymerase zeta from templates containing lesions of ultraviolet radiation and acetylaminofluorene. *Nucleic Acids Res.*, **29**, 2875–2883.

19. Johnson,R.E., Washington,M.T., Haracska,L., Prakash,S. and Prakash,L. (2000) Eukaryotic polymerases iota and zeta act sequentially to bypass DNA lesions. *Nature*, **406**, 1015–1019.

20. Okuda,T., Lin,X., Trang,J. and Howell,S.B. (2005) Suppression of hREV1 expression reduces the rate at which human ovarian carcinoma cells acquire resistance to cisplatin. *Mol. Pharmacol.*, **67**, 1852–1860.

21. Lin,X., Okuda,T., Trang,J. and Howell,S.B. (2006) Human REV1 modulates the cytotoxicity and mutagenicity of cisplatin in human ovarian carcinoma cells. *Mol. Pharmacol.*, **69**, 1748–1754.

22. Ross,A.L., Simpson,L.J. and Sale,J.E. (2005) Vertebrate DNA damage tolerance requires the C-terminus but not BRCT or transferase domains of REV1. *Nucleic Acids Res.*, **33**, 1280–1289.

23. Vaisman,A., Lim,S.E., Patrick,S.M., Copeland,W.C., Hinkle,D.C., Turchi,J.J. and Chaney,S.G. (1999) Effect of DNA polymerases and high mobility group protein 1 on the carrier ligand specificity for translesion synthesis past platinum-DNA adducts. *Biochemistry*, **38**, 11026–11039.

24. Wu,F., Lin,X., Okuda,T. and Howell,S.B. (2004) DNA polymerase zeta regulates cisplatin cytotoxicity, mutagenicity, and the rate of development of cisplatin resistance. *Cancer Res.*, **64**, 8029–8035.

25. Lin,X., Trang,J., Okuda,T. and Howell,S.B. (2006) DNA polymerase zeta accounts for the reduced cytotoxicity and enhanced mutagenicity of cisplatin in human colon carcinoma cells that have lost DNA mismatch repair. *Clin. Cancer Res.*, **12**, 563–568.

26. Hoffmann,J.S., Pillaire,M.J., Garcia-Estefania,D., Lapalu,S. and Villani,G. (1996) In vitro bypass replication of the cisplatin-d(GpG) lesion by calf thymus DNA polymerase beta and human immunodeficiency virus type I reverse transcriptase is highly mutagenic. *J. Biol. Chem.*, **271**, 15386–92.

27. Vaisman,A. and Chaney,S.G. (2000) The efficiency and fidelity of translesion synthesis past cisplatin and oxaliplatin GpG adducts by human DNA polymerase beta. *J. Biol. Chem.*, **275**, 13017–13025.

28. Vaisman,A., Warren,M.W. and Chaney,S.G. (2001) The effect of DNA structure on the catalytic efficiency and fidelity of human DNA polymerase beta on templates with platinum-DNA adducts. *J. Biol. Chem.*, **276**, 18999–19005.

29. Havener,J.M., McElhinny,S.A., Bassett,E., Gauger,M., Ramsden,D.A. and Chaney,S.G. (2003) Translesion synthesis past platinum DNA adducts by human DNA polymerase mu. *Biochemistry*, **42**, 1777–1788.

30. Siddik,Z.H. (2003) Cisplatin: mode of cytotoxic action and molecular basis of resistance. *Oncogene*, **22**, 7265–7279.

31. Boulikas,T. and Vougiouka,M. (2003) Cisplatin and platinum drugs at the molecular level. (Review). *Oncol. Rep.*, **10**, 1663–1682.

32. Chaney,S.G., Campbell,S.L., Bassett,E. and Wu,Y. (2005) Recognition and processing of cisplatin- and oxaliplatin-DNA adducts. *Crit. Rev. Oncol. Hematol.*, **53**, 3–11.

33. Wang,D. and Lippard,S.J. (2005) Cellular processing of platinum anticancer drugs. *Nat. Rev. Drug Discov.*, **4**, 307–320.

34. Rabik,C.A. and Dolan,M.E. (2007) Molecular mechanisms of resistance and toxicity associated with platinating agents. *Cancer Treat Rev.*, **33**, 9–23.

35. Fiala,K.A. and Suo,Z. (2004) Mechanism of DNA polymerization catalyzed by Sulfolobus solfataricus P2 DNA polymerase IV. *Biochemistry*, **43**, 2116–2125.

36. Fiala,K.A. and Suo,Z. (2004) Pre-steady-state kinetic studies of the fidelity of Sulfolobus solfataricus P2 DNA polymerase IV. *Biochemistry*, **43**, 2106–2115.

37. Fiala,K.A., Hypes,C.D. and Suo,Z. (2007) Mechanism of abasic lesion bypass catalyzed by a Y-family DNA polymerase. *J. Biol. Chem.*, **282**, 8188–8198.

38. Reed,E., Ozols,R.F., Tarone,R., Yuspa,S.H. and Poirier,M.C. (1987) Platinum-DNA adducts in leukocyte DNA correlate with disease response in ovarian cancer patients receiving platinum-based chemotherapy. *Proc. Natl Acad. Sci. USA*, **84**, 5024–5028.

39. Reed,E., Ozols,R.F., Tarone,R., Yuspa,S.H. and Poirier,M.C. (1988) The measurement of cisplatin-DNA adduct levels in testicular cancer patients. *Carcinogenesis*, **9**, 1909–1911.

40. Boudsocq,F., Iwai,S., Hanaoka,F. and Woodgate,R. (2001) Sulfolobus solfataricus P2 DNA polymerase IV (Dpo4): an archaeal DinB-like DNA polymerase with lesion-bypass properties akin to eukaryotic poleta. *Nucleic Acids Res.*, **29**, 4607–4616.

41. Suo,Z., Lippard,S.J. and Johnson,K.A. (1999) Single d(GpG)/cis-diammineplatinum(II) adduct-induced inhibition of DNA polymerization. *Biochemistry*, **38**, 715–726.

42. Fiala,K.A., Brown,J.A., Ling,H., Kshetry,A.K., Zhang,J., Taylor,J.S., Yang,W. and Suo,Z. (2007) Mechanism of template-independent nucleotide incorporation catalyzed by a template-dependent DNA polymerase. *J. Mol. Biol.*, **365**, 590–602.

43. de Boer,J.G. and Glickman,B.W. (1989) Sequence specificity of mutation induced by the anti-tumor drug cisplatin in the CHO aprt gene. *Carcinogenesis*, **10**, 1363–1367.

44. Mis,J.R. and Kunz,B.A. (1990) Analysis of mutations induced in the SUP4-o gene of Saccharomyces cerevisiae by cis-diammine dichloroplatinum(II). *Carcinogenesis*, **11**, 633–638.

45. Cariello,N.F., Swenberg,J.A. and Skopek,T.R. (1992) In vitro mutational specificity of cisplatin in the human hypoxanthine guanine phosphoribosyltransferase gene. *Cancer Res.*, **52**, 2866–2873.

46. Pillaire,M.J., Margot,A., Villani,G., Sarasin,A., Defais,M. and Gentil,A. (1994) Mutagenesis in monkey cells of a vector containing

a single d(GPG) cis-diamminedichloroplatinum(II) adduct placed on codon 13 of the human H-ras proto-oncogene. *Nucleic Acids Res.*, **22**, 2519–2524.

47. Louro,H., Silva,M.J. and Boavida,M.G. (2002) Mutagenic activity of cisplatin in the lacZ plasmid-based transgenic mouse model. *Environ. Mol. Mutagen.*, **40**, 283–291.

48. Takahara,P.M., Rosenzweig,A.C., Frederick,C.A. and Lippard,S.J. (1995) Crystal structure of double-stranded DNA containing the major adduct of the anticancer drug cisplatin. *Nature*, **377**, 649–652.

49. Takahara,P.M., Frederick,C.A. and Lippard,S.J. (1996) Crystal structure of the anticancer drug cisplatin bound to duplex DNA. *J. Am. Chem. Soc.*, **118**, 12309–12321.

50. Gelasco,A. and Lippard,S.J. (1998) NMR solution structure of a DNA dodecamer duplex containing a cis-diammineplatinum(II) d(GpG) intrastrand cross-link, the major adduct of the anticancer drug cisplatin. *Biochemistry*, **37**, 9230–9239.

51. Comess,K.M., Burstyn,J.N., Essigmann,J.M. and Lippard,S.J. (1992) Replication inhibition and translesion synthesis on templates containing site-specifically placed cis-diamminedichloroplatinum(II) DNA adducts. *Biochemistry*, **31**, 3975–3990.

52. Mamenta,E.L., Poma,E.E., Kaufmann,W.K., Delmastro,D.A., Grady,H.L. and Chaney,S.G. (1994) Enhanced replicative bypass of platinum-DNA adducts in cisplatin-resistant human ovarian carcinoma cell lines. *Cancer Res.*, **54**, 3500–3505.

53. Canitrot,Y., Cazaux,C., Frechet,M., Bouayadi,K., Lesca,C., Salles,B. and Hoffmann,J.S. (1998) Overexpression of DNA polymerase beta in cell results in a mutator phenotype and a decreased sensitivity to anticancer drugs. *Proc. Natl Acad. Sci. USA*, **95**, 12586–12590.

54. Alt,A., Lammens,K., Chiocchini,C., Lammens,A., Pieck,J.C., Kuch,D., Hopfner,K.P. and Carell,T. (2007) Bypass of DNA lesions generated during anticancer treatment with cisplatin by DNA polymerase eta. *Science*, **318**, 967–970.

55. Yamada,M., O'Regan,E., Brown,R. and Karran,P. (1997) Selective recognition of a cisplatin-DNA adduct by human mismatch repair proteins. *Nucleic Acids Res.*, **25**, 491–496.

56. Fourrier,L., Brooks,P. and Malinge,J.M. (2003) Binding discrimination of MutS to a set of lesions and compound lesions (base damage and mismatch) reveals its potential role as a cisplatin-damaged DNA sensing protein. *J. Biol. Chem.*, **278**, 21267–21275.

57. Washington,M.T., Prakash,L. and Prakash,S. (2003) Mechanism of nucleotide incorporation opposite a thymine-thymine dimer by yeast DNA polymerase eta. *Proc. Natl Acad. Sci. USA*, **100**, 12093–12098.

58. Park,H., Zhang,K., Ren,Y., Nadji,S., Sinha,N., Taylor,J.S. and Kang,C. (2002) Crystal structure of a DNA decamer containing a cis-syn thymine dimer. *Proc. Natl Acad. Sci. USA*, **99**, 15965–15970.

59. Ling,H., Boudsocq,F., Plosky,B.S., Woodgate,R. and Yang,W. (2003) Replication of a cis-syn thymine dimer at atomic resolution. *Nature*, **424**, 1083–1087.